JOC The Journal of Organic Chemistry

pubs.acs.org/joc

Note

Construction of Ribonuclease-Decorated Artificial Virus-like Capsid by Peptide Self-assembly

Kazunori Matsuura,* Junpei Ota, Seiya Fujita, Yuriko Shiomi, and Hiroshi Inaba

Cite This: J. Org. Chem. 2020, 85, 1668−1673

Read Online

ACCESS | Metrics & More | Article Recommendations | Supporting Information

ABSTRACT: Artificial virus-like capsids decorated with ribonuclease S (RNase S) on their exterior were constructed by the self-assembly of β-annulus-S-peptide and the interaction between S-peptide moiety and S-protein. The β-annulus-S-peptide was synthesized by native chemical ligation of β-annulus-SBz peptide with Cys-containing S-peptide that self-assembled into artificial virus-like capsids of approximately 47 nm in size. Reconstruction of RNase S on the artificial virus-like capsids afforded spherical assembly attached small spheres on the surface, which retained ribonuclease activity.

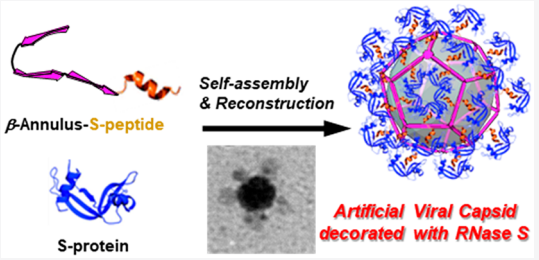

Viral capsids, the outer shells of virus assembled from proteins, have been recognized as attractive organic materials possessing discrete size, unique morphology, and a constant aggregation number. They have been used as nanocarriers, nanotemplates, and nanoreactors.[1−9] Over the past decade, rational design of artificial protein/peptide assemblies based on ligand−receptor interactions, domain swapping, protein−protein interactions, and interactions between secondary structures such as β-sheet and α-helix have permitted the construction of various nanoarchitectures such as fiber, ring, tube, and capsule.[10−23] The secondary structure formation of designed peptide/protein assemblies can be predicted from the primary sequence, and the self-assembly process can also be programmed. Recently, virus-like discrete nanoarchitectures have been constructed by the self-assembly of fusion proteins consisting of symmetric oligomer-forming subunits.[24−29] Yeates et al. demonstrated that fusion proteins comprising trimer- and dimer-forming units self-assembled into cubic protein assemblies.[24] Kawakami et al. designed fusion proteins consisting of pentamer- and dimer-forming coiled-coil units, which self-assembled into polyhedral protein cages.[27] Although these virus-like protein assemblies are expected to apply to nanomaterials, the functionalization of nanocapsules remains challenging.

We have developed a simpler strategy compared with the ones used to date of constructing a virus-like nanoarchitecture using peptide self-assembly. We found that the 24-mer β-annulus peptide (INHVGGTGGAIMAPVAVTRQLVGS), which participates in the formation of a dodecahedral internal skeleton of tomato bushy stunt virus,[30,31] spontaneously self-assembled into "artificial virus-like capsid" with a size of 30−50 nm.[32] In the cationic interior of the artificial virus-like capsid, anionic guests such as anionic dyes, DNAs, and quantum dots can be encapsulated.[14,33,34] The N-terminal modification of β-annulus peptide with Ni-NTA enabled encapsulation of His-tag GFP in the artificial virus-like capsid,[35] as the N-terminus is expected to be directed to the interior of capsid by ζ-potential measurement.[33] Modification of the C-terminus, expected to be directed to the exterior of capsid, enabled the surface modification of artificial virus-like capsids with gold nanoparticles, coiled-coil peptides, single-stranded DNAs, and human serum albumin (HSA).[14,36,37] HSA-modified β-annulus peptide was synthesized by linking Cys-residues of HSA and β-annulus peptide with bis-maleimide linker, and the resulting conjugate self-assembled into a stable artificial virus-like capsid displaying HSA on the surface.[37] Thus, the modification of large protein to β-annulus peptide did not prevent the self-assembly into artificial virus-like capsid.

Some naturally occurring viruses have enzymes on the surface. For example, the influenza virus has neuraminidase, which hydrolyzes sialic acid from oligosaccharides. Although viral capsids armed with enzymes have potential as a nanodevice in a cell, there is only one reports on the construction of enzyme-modified natural viral capsids.[38] Here, we demonstrate the first example of construction of enzyme-decorated artificial virus-like capsid self-assembled from β-annulus peptide.

Ribonuclease S (RNase S) is known as a split-type enzyme that can be reconstructed from S-protein and S-peptide.[39,40] Therefore, RNase S has been utilized as a reversible building block of supramolecular assemblies bearing enzymatic activity.[41−44] We designed β-annulus peptide bearing an S-peptide at the C-terminus (β-annulus-S-peptide) that was synthesized by native chemical ligation (NCL) of the

Special Issue: Modern Peptide and Protein Chemistry

Received: August 23, 2019
Published: December 25, 2019

https://dx.doi.org/10.1021/acs.joc.9b02295
J. Org. Chem. 2020, 85, 1668−1673

Scheme 1. (A) Synthesis of β-Annulus-S-peptide by Native Chemical Ligation. (B) Construction of Artificial Virus-like Capsids Decorated with S-Peptide and RNase S

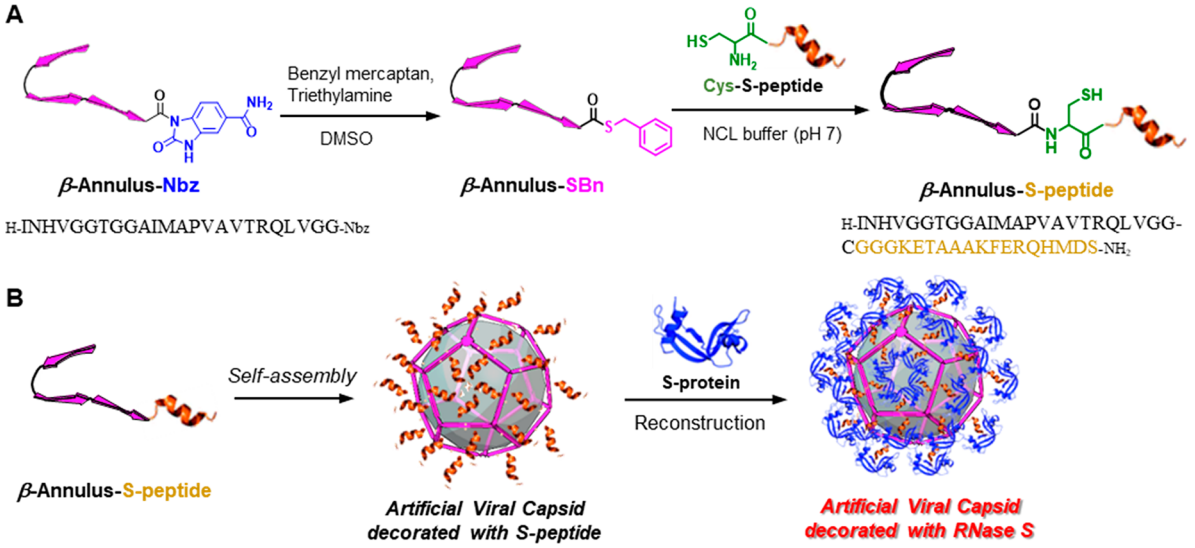

benzylthioesterified β-annulus peptide at the C-terminus (β-annulus-SBz) with an S-peptide[45] bearing Cys at the N-terminus (Cys-S-peptide: CGGGKETAAAKFERQHMDS) as shown in Scheme 1A. As the C-terminus of β-annulus peptide can be directed to the exterior of an artificial virus-like capsid,[33] we expected that the artificial virus-like capsid decorated with RNase S would be constructed by the self-assembly of β-annulus-S-peptide followed by an interaction of S-protein with the S-peptide moiety at the outer surface (Scheme 1B).

In the past, we have successfully synthesized β-annulus peptide bearing coiled-coil-forming peptide at C-terminus[36] by Dawson's NCL using peptides activated by an *N*-acylbenzimidazolinone (Nbz) group at the C-terminus synthesized by Fmoc-solid phase synthesis.[46] Similarly, we planned to synthesize β-annulus-S-peptide by Dawson's NCL method. β-Annulus-Nbz was synthesized by an Fmoc method on commercially available Dawson Dbz AM resin and then converted to β-annulus-SBn by benzyl mercaptan and trimethylamine (Scheme 1A). The crude β-annulus-SBn peptide obtained was used for the synthesis of the β-annulus-S-peptide by NCL without purification. β-Annulus-SBn peptide and 1.5 equiv of Cys-S-peptide were mixed and incubated in NCL buffer containing 4-mercaptophenylacetic acid (MPAA) as thioester catalysis for 1 h at 37 °C. The reversed-phase HPLC chart of the reaction mixture revealed that peaks assigned to the β-annulus-SBn peptide and the Cys-S-peptide disappeared and a new peak appeared (Figure S1). The β-annulus-S-peptide was purified by reversed-phase HPLC and confirmed by MALDI-TOF MS (m/z = 4280 $[M]^+$, Figure S2).

The complexation of S-protein to the β-annulus-S-peptide to reconstruct RNase S was confirmed by CD spectra. It is known that the negative molar ellipticity of S-protein at 215−235 nm is increased by complexing with S-peptide (Figure S3).[47] Similarly, complexing S-protein with an equimolar concentration of β-annulus-S-peptide increased the negative molar ellipticity of S-protein (Figure 1). The molar ellipticity of an S-protein/β-annulus-S-peptide was approximately equal to that of an S-protein/S-peptide complex. These results indicate that β-annulus peptide is minimally affected by the reconstruction of RNase S. Since the amount of change of CD spectra are too small to evaluate strictly the dissociation constant of RNase S, we are planning to evaluate it using isothermal titration calorimetry in near future study.

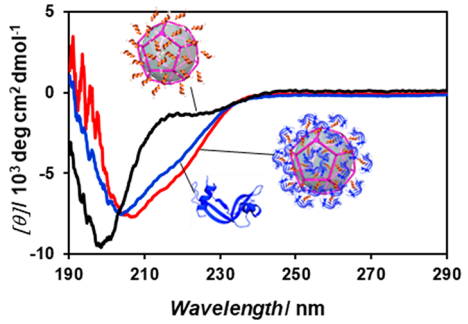

Figure 1. CD spectra of the 25 μM β-annulus-S-peptide (black), 25 μM S-protein (blue), and their equimolar mixture (red) at [β-annulus-S-peptide] = [S-protein] = 25 μM in 10 mM ammonium acetate buffer (pH 4.5) at 25 °C.

The average diameter obtained from dynamic light scattering (DLS) measurement of the 25 μM β-annulus-S-peptide solution showed an assembly with the size of 47 ± 21 nm (Figure 2A). This size is comparable to that of the artificial virus-like capsid self-assembled from the unmodified β-annulus peptide (48 ± 13 nm).[32] Transmission electron microscopy (TEM) image showed that β-annulus-S-peptide self-assembled into spherical structures with sizes ranging from 40 to 80 nm (Figure 2D). Both DLS and TEM showed that intact S-protein did not self-assemble at 25 μM (Figure 2B,E). On the contrary, the DLS of an equimolar mixture of β-annulus-S-peptide and S-protein showed the formation of an assembly with the size of 51 ± 32 nm (Figure 2C). In the TEM image of the equimolar mixture of β-annulus-S-peptide and S-protein, we observed spherical assemblies with the size of 50−65 nm attached small spheres of 5−10 nm on the surface (Figure 2F). The small spheres may be ascribed to RNase S on the capsid surface. Considered together with the CD spectra (Figure 1), these results indicate that the reconstruction of RNase S on the artificial virus-like capsid minimally influenced the self-assembling behavior. It is known that the association constant

https://dx.doi.org/10.1021/acs.joc.9b02295
J. Org. Chem. 2020, 85, 1668−1673

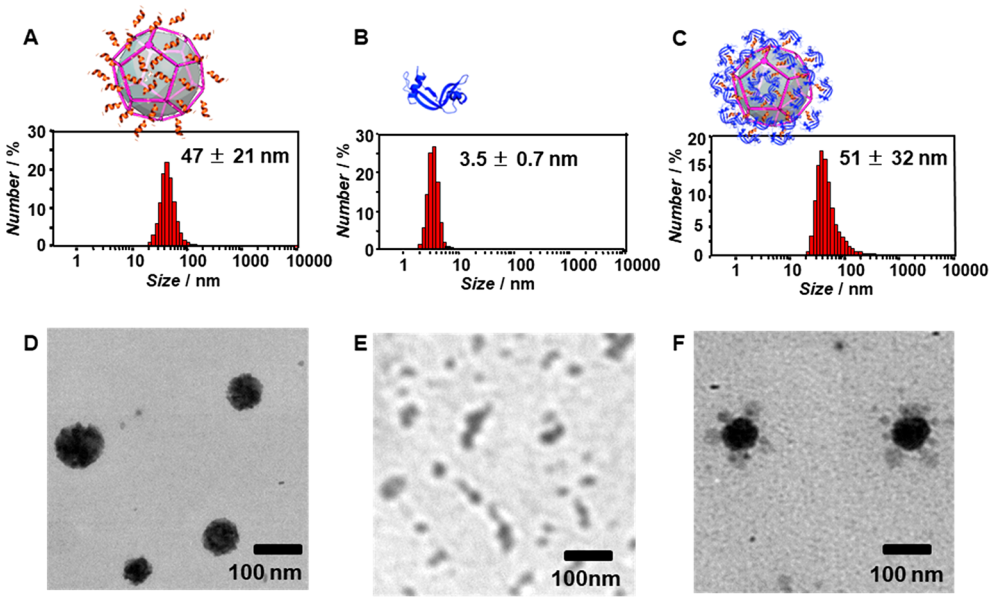

Figure 2. Size distributions obtained from DLS (A–C) and TEM images (D–F) for solutions of 25 μM β-annulus-S-peptide (A, D), 25 μM S-protein (B, E), and their equimolar mixture (C, F) at [β-annulus-S-peptide] = [S-protein] = 25 μM in 10 mM ammonium acetate buffer (pH 4.5) at 25 °C. TEM samples were stained with sodium phosphotungstate.

between S-protein and S-peptide is 7×10^6 M^{-1} at 25 °C.[40] Thus, we can calculate that about 92% of S-protein was reconstructed on the S-peptide-displayed capsid at [β-annulus-S-peptide] = [S-protein] = 25 μM. Since one artificial virus-like capsid ideally consists of 60 β-annulus peptides, the average number of RNase S on the capsid can be estimated to be 55. We are planning to evaluate the exact number of the RNase S on the capsid by using chromophore-labeled S-protein or gold-labeled anti-RNase antibody in near future study.

We measured the ζ-potentials of the RNase S, S-peptide-expressing capsid and RNase-expressing capsid at pH 4.5 to confirm that RNase was displayed on the exterior of the artificial virus-like capsids (Figure 3). The ζ-potential of S-peptide-decorated capsid was 14.4 ± 5.3 mV, whereas that of RNase-decorated capsid was 31.7 ± 6.5 mV which is close to that of intact RNase S, 26.2 ± 11.9 mV. The results indicate that RNase S molecules were displayed on the outer surface of the artificial virus-like capsid. The enzymatic activity of RNase S on the artificial virus-like capsid was estimated by fluorimetric assay using RNaseAlert Lab Test Kit (Thermo Fisher Scientific), in which fluorescence intensity of RNA substrate is enhanced by cleaving the RNA strand with ribonuclease. The fluorescence intensity in the presence of S-protein or S-peptide-decorated capsid was low, indicating less enzymatic activity. In contrast, the fluorescence intensity in the presence of RNase S-decorated capsid reached up to 85% activity of intact RNase S, despite the crowded surface environment (Figure 4). Therefore, we have successfully

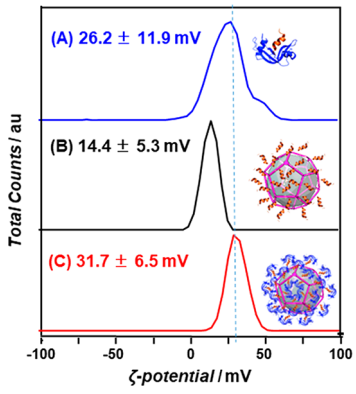

Figure 3. ζ-Potentials of (A) 25 μM RNase S, (B) assembly of 25 μM β-annulus-S-peptide, and (C) coassembly of 25 μM β-annulus-S-peptide and 25 μM S-protein in 10 mM ammonium acetate buffer (pH 4.5) at 25 °C.

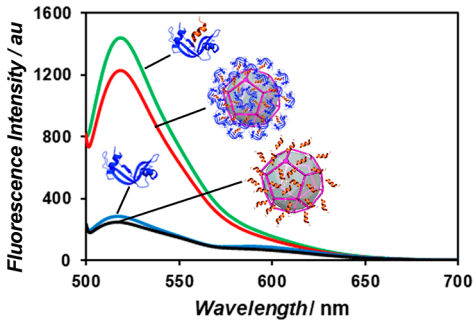

Figure 4. Fluorescence spectra of reaction mixture using RNaseAlert Lab Test Kit in the presence of RNase S (green), RNase-decorated artificial virus-like capsid (red), S-protein (blue), and S-peptide-decorated artificial virus-like capsid (black) in 10 mM ammonium acetate buffer (pH 4.5) at 25 °C. [RNase S] = [β-annulus-S-peptide] = [S-protein] = 25 μM; the excitation wavelength was 490 nm.

constructed an artificial virus-like capsid having enzymatic activity. The size distribution and ribonuclease activity of RNase S-decorated artificial virus-like capsid were almost retained for 1 week at least (Figure S4). Ribonuclease has potential application in anticancer therapy;[48] thus, we envisage that the RNase-decorated artificial virus-like capsid can be applied to an anticancer nanodevice with both ribonuclease activity and drug delivery ability.

In conclusion, we demonstrated the construction of an artificial virus-like capsid decorated with RNase S by the self-

https://dx.doi.org/10.1021/acs.joc.9b02295
J. Org. Chem. 2020, 85, 1668–1673

assembly of a β-annulus peptide bearing an S-peptide followed by interaction of the S-protein with the S-peptide moiety at the surface. DLS and TEM of the RNase-decorated artificial virus-like capsid revealed the formation of spherical assembly with the size of 50−65 nm attached small spheres of 5−10 nm on the surface. The RNase-decorated artificial virus-like capsid sufficiently retained the ribonuclease activity despite the crowded environment at the surface. Detail experiments of the thermal stability of RNase S-decorated artificial virus-like capsid are currently in progress. The strategy for protein display on artificial virus-like capsids using reconstruction of a split-protein would be a novel approach for the construction of nanoarchitecture comprised of multiple proteins, which is applied to cascade enzymatic reactions.

EXPERIMENTAL SECTION

General Methods. Reversed-phase HPLC was performed at ambient temperature using a Shimadzu LC-6AD liquid chromatography system equipped with a UV/vis detector (220 nm, Shimadzu SPD-10AVvp) and Inertsil ODS-3 or WP300 C4 (GL Science) columns (250 × 4.6 mm or 250 × 20 mm). MALDI-TOF mass spectra were obtained using an Autoflex III instrument (Bruker Daltonics) in linear/positive mode with α-cyano-4-hydroxy cinnamic acid (α-CHCA) or sinapinic acid as a matrix. CD spectra were taken at 25 °C in a 1.0 mm quartz cell using a JASCO J-820 spectrophotometer equipped with a Peltier-type thermostatic cell holder. Ribonuclease S from bovine pancreas was purchased from Sigma-Aldrich and separated into the S-peptide and S-protein using reversed-phase HPLC with a Inertsil WP300 C4 (GL Science) column according to the literature.[42] Other reagents were obtained from commercial sources and were used without further purification. Deionized water of high resistivity (>18 MΩ cm) was purified using a Millipore Purification System (Milli-Q water) and was used as a solvent for the present peptides.

Synthesis of β-Annulus-Nbz Peptide. The β-annulus peptide functionalized at the C-terminus with an *N*-acylbenzimidazolinone (H-INHVGGTGGAIMAPVAVTRQLVGG-Nbz) was synthesized at the 0.10 mmol scale on commercially available Dawson Dbz AM resin (Merck Millipore) using microwave-assisted Fmoc-based coupling reactions. The amino group of the resin was protected by allyloxycarbonate (Alloc) with a mixture of 3.5 equiv of allylchloroformate and 1 equiv of diisopropylethylamine (DIPEA) at room temperature for 24 h. The Fmoc group was deprotected using 20% piperidine in *N*,*N*-dimethylformamide (DMF) at room temperature for 15 min. Fmoc-protected amino acids (4 equiv) were coupled using (1-cyano-2-ethoxy-2-oxoethylidenaminooxy)dimethylamino-morpholinocarbenium hexafluorophosphate (COMU, 4 equiv) in *N*-methylpyrrolidone (NMP) as the activating agent and DIPEA (8 equiv) in NMP as the base. Coupling reactions were carried out using a microwave synthesizer (Biotage Initiator+) for 5 min at 25 W at a maximum temperature of 75 °C throughout the synthesis. Progression of the coupling reaction and Fmoc deprotection was confirmed by TNBS and chloranil test kit (Tokyo Chemical Industry Co., Ltd.). After loading of the amino acid, deprotection of the Alloc group was carried out using a mixture of 20 equiv of $PhSiH_3$ and 0.35 equiv of $Pd(PPh_3)_4$ in CH_2Cl_2 for 30 min. Next, the resin was treated with 5 equiv of *p*-nitrophenylchloroformate in CH_2Cl_2 for 1 h that was followed by treatment with 0.5 M DIPEA in DMF for 30 min to convert the Nbz group. The peptide was deprotected and cleaved from the resin by treatment with a cleavage cocktail of trifluoroacetic acid (TFA)/1,2-ethanedithiol/triisopropylsilane/water (2.93/0.078/0.031/0.078 (mL), respectively) at room temperature for 3 h. Reaction mixtures were filtered to remove resins, and filtrates were concentrated under a vacuum. The peptide was precipitated by adding methyl *tert*-butyl ether (MTBE) to the residue, and the supernatant was decanted. After three washes with MTBE, the crude peptide was lyophilized to give 61.3 mg of a flocculent solid (45.9% yield). The reversed-phase HPLC of the crude peptide eluting with a linear gradient of CH_3CN/water containing 0.1% TFA (5/95 to 100/0 over 95 min) showed one peak at 30.4 min. MALDI-TOF MS (matrix: α-CHCA): m/z = 2436 $[M + H]^+$.

Synthesis of Cys-S-peptide. The S-peptide bearing CGGG sequence at N-terminus (H-CGGGKETAAAKFERQHMDS-NH_2) was synthesized at the 0.125 mmol scale on commercially available Rink amide resin (Watanabe Chemical Industry, Ltd.) using microwave-assisted Fmoc-based coupling reactions. Fmoc deprotection was achieved using 20% piperidine in DMF. Coupling reactions were carried out using an NMP solution containing COMU (4 equiv) and DIPEA (8 equiv) in 25 W microwave (Biotage Initiator$^+$) for 5 min at 75 °C. The peptide was deprotected and cleaved from the resin by treatment with a cleavage cocktail at room temperature for 3 h. Reaction mixtures were filtered to remove resins, and the filtrates were concentrated under a vacuum. The peptide was precipitated by adding MTBE to the residue, and the supernatant was decanted. After three washes with MTBE, the precipitated peptide was dried in vacuo. The crude product was purified by reversed-phase HPLC eluting with a linear gradient of CH_3CN/water containing 0.1% TFA (5/95 to 100/0 over 95 min). The fraction containing the desired Cys-S-peptide was lyophilized to give a flocculent solid (21.1% yield). MALDI-TOF MS (matrix: α-CHCA): m/z = 2023 $[M + H]^+$.

Synthesis of β-Annulus-S-peptide by NCL. Crude β-annulus-Nbz peptide powder was added to a mixture of 10% benzylmercaptan and 20 mM triethylamine in DMSO, and the solution was incubated at 37 °C for 15 min to convert to the β-annulus-SBz peptide. The β-annulus-SBz peptide was precipitated by adding ethyl acetate to the reaction mixture, and the supernatant was decanted. After three washes with ethyl acetate, the precipitated peptide was dried in vacuo. The precipitated peptide was used for NCL without further purification (crude yield: 51.7%). MALDI-TOF MS (matrix: α-CHCA): m/z = 2381 $[M]^+$.

NCL buffer (pH 7.0) was prepared by dissolving 6 M guanidinium hydrochloride, 20 mM triscarboxyethyl phosphine (TCEP), 200 mM 4-mercaptophenylacetic acid (MPAA), and 200 mM sodium phosphate in water and degassed with N_2. The β-annulus-SBn (1 mM) and the Cys-S-peptide (1.5 mM) were dissolved in NCL buffer, and the mixture was incubated at 37 °C for 1 h. The reaction mixture was purified by reversed-phase HPLC eluted with a linear gradient of CH_3CN/water containing 0.1% TFA (5/95 to 100/0 over 95 min). The isolated β-annulus-S-peptide was lyophilized to give a flocculent solid (13.4% yield). MALDI-TOF MS (matrix: α-CHCA): m/z = 4280 $[M]^+$.

DLS and ζ-Potential. Stock solutions (0.1 mM) of β-annulus-S-peptide were prepared by dissolution in 10 mM ammonium acetate buffer (pH 4.5) followed by sonication for 5 min. The samples were prepared by diluting the stock solutions with 10 mM ammonium acetate buffer (pH 4.5) or mixing with S-protein in the same buffer and were then incubated at 25 °C for 1 h. The DLS measurements were carried out using a Zetasizer Nano ZS (MALVERN) instrument with an incident He−Ne laser (633 nm) at 25 °C. Correlation times of the scattered light intensities $G(\tau)$ were measured several times and the means were calculated for the diffusion coefficient. Hydrodynamic diameters of the scattering particles were calculated using the Stokes−Einstein equation. Zeta potentials of β-annulus-S-peptide, S-protein, and their mixture at 25 μM in 10 mM ammonium acetate buffer (pH 4.5) were measured at 25 °C using a Zetasizer Nano ZS (MALVERN) with a DT1061 clear disposable zeta cell.

TEM. Aliquots (3 μL) of the DLS samples were applied to hydrophilized carbon-coated Cu-grids (C-SMART Hydrophilic TEM grids, ALLANCE Biosystems) for 1 min and then removed using filter paper. Subsequently, the TEM grids were instilled in the staining solution, 2% phosphotungstic acid $(Na_3(PW_{12}O_{40})\ (H_2O)_n)$ (3 μL), for 1 min, and then removed using filter paper. After the sample-loaded carbon-coated grids were dried in vacuo, they were analyzed by TEM (JEOL JEM 1400 Plus) using an accelerating voltage of 80 kV.

Ribonuclease Assay. The ribonuclease activity of RNase-decorated artificial virus-like capsid was measured by fluorescence spectroscopy using RNaseAlert Lab Test Kit (Thermo Fisher Scientific). A solution

https://dx.doi.org/10.1021/acs.joc.9b02295
J. Org. Chem. 2020, 85, 1668−1673

of fluorescent RNA substrate in 10× RNaseAlert Lab Test buffer (5 μL) was added to a solution of β-annulus-S-peptide (25 μM) and S-protein (25 μM) in 10 mM ammonium acetate buffer (pH 4.5) and this mixture was vortexed. After incubation at 37 °C for 1 h, the mixture was diluted with 10 mM ammonium acetate buffer (150 μL). The fluorescence spectrum of the mixture was measured using JASCO FP-8200 spectrofluorometer at 25 °C at an excitation wavelength of 490 nm.

■ ASSOCIATED CONTENT

Supporting Information

The Supporting Information is available free of charge at https://pubs.acs.org/doi/10.1021/acs.joc.9b02295.

Reversed-phase HPLC charts of NCL reaction mixture, MALDI-TOF-MS of the purified β-annulus-S-peptide, CD spectra of reconstructed RNase S, and time course of the size distribution and retained ribonuclease activity of RNase S-decorated artificial virus-like capsid (PDF)

■ AUTHOR INFORMATION

Corresponding Author

Kazunori Matsuura − *Tottori University, Tottori, Japan;* orcid.org/0000-0001-5472-7860; Phone: +81 857-31-5262; Email: ma2ra-k@tottori-u.ac.jp

Other Authors

Junpei Ota − *Tottori University, Tottori, Japan*

Seiya Fujita − *Tottori University, Tottori, Japan*

Yuriko Shiomi − *Tottori University, Tottori, Japan*

Hiroshi Inaba − *Tottori University, Tottori, Japan;* orcid.org/0000-0002-7658-7827

Complete contact information is available at: https://pubs.acs.org/10.1021/acs.joc.9b02295

Notes

The authors declare no competing financial interest.

■ ACKNOWLEDGMENTS

This research was partially supported by The Asahi Glass Foundation and a Grant-in-Aid for Scientific Research on Innovative Areas "Chemistry for Multimolecular Crowding Biosystems" (JSPS KAKENHI Grant No. JP18H04558).

■ REFERENCES

(1) *Viral Nanotechnology*; Khudyakov, Y., Pumpens, P., Eds.; CRC Press, 2016.

(2) Douglas, T.; Young, M. Viruses: Making friends with old foes. *Science* **2006**, *312*, 873−875.

(3) Steinmetz, N. F.; Evans, D. J. Utilisation of plant viruses in bionanotechnology. *Org. Biomol. Chem.* **2007**, *5*, 2891−2902.

(4) Papapostolou, D.; Howorka, S. Engineering and exploiting protein assemblies in synthetic biology. *Mol. BioSyst.* **2009**, *5*, 723−732.

(5) Witus, L. S.; Francis, M. B. Using synthetically modified proteins to make new materials. *Acc. Chem. Res.* **2011**, *44*, 774−783.

(6) Bronstein, L. M. Virus-based nanoparticles with inorganic cargo: What does the future hold? *Small* **2011**, *7*, 1609−1618.

(7) Azuma, Y.; Edwardson, T. G. W.; Hilvert, D. Tailoring lumazine synthase assemblies for bionanotechnology. *Chem. Soc. Rev.* **2018**, *47*, 3543−3557.

(8) van Rijn, P.; Schirhagl, R. Viruses, artificial viruses and virus-based structures for biomedical applications. *Adv. Healthcare Mater.* **2016**, *5*, 1386−1400.

(9) Schwarz, B.; Madden, P.; Avera, J.; Gordon, B.; Larson, K.; Miettinen, H. M.; Uchida, M.; LaFrance, B.; Basu, G.; Rynda-Apple, A.; Douglas, T. Symmetry controlled, genetic presentation of bioactive proteins on the P22 virus-like particle using an external decoration protein. *ACS Nano* **2015**, *9*, 9134−9147.

(10) Matsuurua, K. Rational design of self-assembled proteins and peptides for nano- and micro-sized architectures. *RSC Adv.* **2014**, *4*, 2942−2953.

(11) Ramakers, B. E. I.; van Hest, J. C. M.; Löwik, D. W. P. M. Molecular tools for the construction of peptide-based materials. *Chem. Soc. Rev.* **2014**, *43*, 2743−2756.

(12) De Santis, E.; Ryadnov, M. G. Peptide self-assembly for nanomaterials: the old new kid on the block. *Chem. Soc. Rev.* **2015**, *44*, 8288−8300.

(13) Raymond, D. M.; Nilsson, B. L. Multicomponent peptide assemblies. *Chem. Soc. Rev.* **2018**, *47*, 3659−3720.

(14) Matsuura, K. Synthetic approaches to construct viral capsid-like spherical nanomaterials. *Chem. Commun.* **2018**, *54*, 8944−8959.

(15) Lou, S.; Wang, X.; Yu, Z.; Shi, L. Peptide tectonics: Encoded structural complementarity dictates programmable self-assembly. *Adv. Sci.* **2019**, *6*, 1802043.

(16) Fletcher, J. M.; Harniman, R. L.; Barnes, Fr. R. H.; Boyle, A. L.; Collins, A.; Mantell, J.; Sharp, T. H.; Antognozzi, M.; Booth, P. J.; Linden, N.; Miles, M. J.; Sessions, R. B.; Verkade, P.; Woolfson, D. N. Self-assembling cages from coiled-coil peptide modules. *Science* **2013**, *340*, 595−599.

(17) Mosayebi, M.; Shoemark, D. K.; Fletcherd, J. M.; Sessions, R. B.; Lindena, N.; Woolfson, D. N.; Liverpool, T. B. Beyond icosahedral symmetry in packings of proteins in spherical shells. *Proc. Natl. Acad. Sci. U. S. A.* **2017**, *114*, 9014−9019.

(18) Ross, J. F.; Bridges, A.; Fletcher, J. M.; Shoemark, D.; Alibhai, D.; Bray, H. E. V.; Beesley, J. L.; Dawson, W. M.; Hodgson, L. R.; Mantell, J.; Verkade, P.; Edge, C. M.; Sessions, R. B.; Tew, D.; Woolfson, D. N. Decorating self-assembled peptide cages with proteins. *ACS Nano* **2017**, *11*, 7901−7914.

(19) Yang, L.; Liu, A.; Cao, S.; Putri, R. M.; Jonkheijm, P.; Cornelissen, J. J. L. M. Self-assembly of proteins: Towards supramolecular materials. *Chem. - Eur. J.* **2016**, *22*, 15570−15582.

(20) Luo, Q.; Hou, C.; Bai, Y.; Wang, R.; Liu, J. Protein assembly: Versatile approaches to construct highly ordered nanostructures. *Chem. Rev.* **2016**, *116*, 13571−13632.

(21) Sun, H.; Luo, Q.; Hou, C.; Liu, J. Nanostructures based on protein self-assembly: From hierarchical construction to bioinspired materials. *Nano Today* **2017**, *14*, 16−41.

(22) Kuan, S. L.; Bergamini, F. R. G.; Weil, T. Functional protein nanostructures: a chemical toolbox. *Chem. Soc. Rev.* **2018**, *47*, 9069−9105.

(23) Sasaki, E.; Böhringer, D.; van de Waterbeemd, M.; Leibundgut, M.; Zschoche, R.; Heck, A. J. R.; Ban, N.; Hilvert, D. Structure and assembly of scalable porous protein cages. *Nat. Commun.* **2017**, *8*, 14663.

(24) Lai, Y. T.; Tsai, K. L.; Sawaya, M. R.; Asturias, F. J.; Yeates, T. O. Structure and flexibility of nanoscale protein cages designed by symmetric self-assembly. *J. Am. Chem. Soc.* **2013**, *135*, 7738−7743.

(25) Lai, Y. T.; Reading, E.; Hura, G. L.; Tsai, K.-L.; Laganowsky, A.; Asturias, F. J.; Tainer, J. A.; Robinson, C. V.; Yeates, T. O. Structure of a designed protein cage that self-assembles into a highly porous cube. *Nat. Chem.* **2014**, *6*, 1065−1071.

(26) Hsia, Y.; Bale, J. B.; Gonen, S.; Shi, D.; Sheffler, W.; Fong, K. K.; Nattermann, U.; Xu, C.; Huang, P.-S.; Ravichandran, R.; Yi, S.; Davis, T. N.; Gonen, T.; King, N. P.; Baker, D. Design of a hyperstable 60-subunit protein icosahedron. *Nature* **2016**, *535*, 136−139.

(27) Kawakami, N.; Kondo, H.; Matsuzawa, Y.; Hayasaka, K.; Nasu, E.; Sasahara, K.; Arai, R.; Miyamoto, K. Design of hollow protein nanoparticles with modifiable interior and exterior surfaces. *Angew. Chem., Int. Ed.* **2018**, *57*, 12400−12404.

(28) Cristie-David, A. S.; Chen, J.; Nowak, D. B.; Bondy, A. L.; Sun, K.; Park, S. I.; Holl, M. M. B.; Su, M.; Marsh, E. N. G. Coiled-coil-

mediated assembly of an icosahedral protein cage with extremely high thermal and chemical stability. *J. Am. Chem. Soc.* **2019**, *141*, 9207−9216.
(29) Malay, A. D.; Miyazaki, N.; Biela, A.; Chakraborti, S.; Majsterkiewicz, K.; Stupka, I.; Kaplan, C. S.; Kowalczyk, A.; Piette, B. M. A. G.; Hochberg, G. K. A.; Wu, D.; Wrobel, T. P.; Fineberg, A.; Kushwah, M. S.; Kelemen, M.; Vavpetič, P.; Pelicon, P.; Kukura, P.; Benesch, J. L. P.; Iwasaki, K.; Heddle, J. G. An ultra-stable gold-coordinated protein cage displaying reversible assembly. *Nature* **2019**, *569*, 438−442.
(30) Olson, A. J.; Bricogne, G.; Harrison, S. C. Structure of tomato bushy stunt virus IV. The virus particle at 2.9 A resolution. *J. Mol. Biol.* **1983**, *171*, 61−93.
(31) Hopper, P.; Harrison, S. C.; Sauer, R. T. Structure of tomato bushy stunt virus. V. Coat protein sequence determination and its structural implications. *J. Mol. Biol.* **1984**, *177*, 701−713.
(32) Matsuura, K.; Watanabe, K.; Sakurai, K.; Matsuzaki, T.; Kimizuka, N. Self-assembled synthetic viral capsids from a 24-mer viral peptide fragment. *Angew. Chem., Int. Ed.* **2010**, *49*, 9662−9665.
(33) Matsuura, K.; Watanabe, K.; Matsushita, Y.; Kimizuka, N. Guest-binding behavior of peptide nanocapsules self-assembled from viral peptide fragments. *Polym. J.* **2013**, *45*, 529−534.
(34) Nakamura, Y.; Inaba, H.; Matsuura, K. Construction of artificial viral capsids encapsulating short DNAs via disulfide bonds and controlled release of DNAs by reduction. *Chem. Lett.* **2019**, *48*, 544−546.
(35) Matsuura, K.; Nakamura, T.; Watanabe, K.; Noguchi, T.; Minamihata, K.; Kamiya, N.; Kimizuka, N. Self-assembly of Ni-NTA-modified M-annulus peptides into artificial viral capsids and encapsulation of His-tagged proteins. *Org. Biomol. Chem.* **2016**, *14*, 7869−7874.
(36) Fujita, S.; Matsuura, K. Self-assembled artificial viral capsids bearing coiled-coils at the surface. *Org. Biomol. Chem.* **2017**, *15*, 5070−5077.
(37) Matsuura, K.; Honjo, T. Artificial viral capsid dressed up with human serum albumin. *Bioconjugate Chem.* **2019**, *30*, 1636−1641.
(38) Cayetano-Cruz, M.; Coffeen, C. F.; Valadez-García, J.; Montiel, C.; Bustos-Jaimes, I. Decoration of virus-like particles with an enzymatic activity of biomedical interest. *Virus Res.* **2018**, *255*, 1−9.
(39) Richards, F. M.; Vithayathil, P. J. The Preparation of subtilisin-modified ribonuclease and the separation of the peptide and protein components. *J. Biol. Chem.* **1959**, *234*, 1459−1465.
(40) Raines, R. T. Ribonuclease A. *Chem. Rev.* **1998**, *98*, 1045−1066.
(41) Aubin, M. E.; Morales, D. G.; Schifferli, K. H. Labeling ribonuclease S with a 3 nm Au nanoparticle by two-step assembly. *Nano Lett.* **2005**, *5*, 519−522.
(42) Bastings, M. M. C.; de Greef, T. F. A.; van Dongen, J. L. J.; Merkx, M.; Meijer, E. W. Macrocyclization of enzyme-based supramolecular polymers. *Chem. Sci.* **2010**, *1*, 79−88.
(43) Appel, W. P.; Meijer, E. W.; Dankers, P. Y. Enzymatic activity at the surface of biomaterials via supramolecular anchoring of peptides: the effect of material processing. *Macromol. Biosci.* **2011**, *11*, 1706−1712.
(44) DiMaio, J. T. M.; Raymond, D. M.; Nilsson, B. L. Display of functional proteins on supramolecular peptide nanofibrils using a split-protein strategy. *Org. Biomol. Chem.* **2017**, *15*, 5279−5283.
(45) Kim, J. S.; Raines, R. T. Ribonuclease S-peptide as a carrier in fusion proteins. *Protein Sci.* **1993**, *2*, 348−356.
(46) Blanco-Canosa, J. B.; Dawson, P. E. An efficient Fmoc-SPPS approach for the generation of thioester peptide precursors for use in native chemical ligation. *Angew. Chem., Int. Ed.* **2008**, *47*, 6851−6855.
(47) Simons, E. R.; Blout, E. R. Circular dichroism of ribonuclease A, ribonuclease S, and some fragments. *J. Biol. Chem.* **1968**, *243*, 218−221.
(48) Ardelt, W.; Ardelt, B.; Darzynkiewicz, Z. Ribonucleases as potential modalities in anticancer therapy. *Eur. J. Pharmacol.* **2009**, *625*, 181−189.

https://dx.doi.org/10.1021/acs.joc.9b02295
J. Org. Chem. 2020, 85, 1668−1673